academicJournals

Vol. 16(36), pp. 1819-1825, 6 September, 2017
DOI: 10.5897/AJB2017.15967
Article Number: 8E8B2BA65873
ISSN 1684-5315

http://www.academicjournals.org/AJB

African Journal of Biotechnology

Full Length Research Paper

Production, optimization and characterization of silver oxide nanoparticles using *Artocarpus heterophyllus* rind extract and their antifungal activity

Velu Manikandan[1], Pyong-In Yi[2], Palanivel Velmurugan[1], Palaniyappan Jayanthi[3], Sung-Chul Hong[2], Seong-Ho Jang[2], Jeong-Min Suh[2] and Subpiramaniyam Sivakumar[2]*

[1]Division of Biotechnology, Advanced Institute of Environment and Bioscience, College of Environmental and Bioresource Sciences, Chonbuk National University, Iksan, Jeonbuk 54596, South Korea.
[2]Department of Bioenvironmental Energy, College of Natural Resource and Life Science, Pusan National University, Miryang-si, Gyeongsangnam-do, 627-706, Republic of Korea.
[3]Department of Environmental Science, Periyar University, Salem, 636011, Tamil Nadu, India.

Received 1 March, 2017; Accepted 16 May, 2017

For the first time, the phytochemical fabrication of noble silver oxide nanoparticles was reported using *Artocarpus heterophyllus* rind extract as well as their characterization. The UV-vis absorption spectrum of the phytochemical-mediated reduced reaction mixture showed a surface plasmon peak at 428 nm, which confirmed the presence of silver nanoparticles. The silver nanoparticle production was ideal at pH 9 with 2.0 mL jackfruit rind extract, Ag^+ 1.0 mM and 180 min of reaction time. Fourier transform infrared spectroscopy analysis indicated the presence of acids, esters, alcohols, pyrazine, etc. which can act as capping agents around the nanoparticles. X-ray diffraction analysis confirmed the face-centered cubic crystalline and the oxygen structure of metallic silver nanoparticles. The average diameter of silver nanoparticles is ~17 nm via high resolution transmission electron microscopy, which agrees with the average crystallite size (24.2 nm) calculated from X-ray diffraction analysis and selected area electron diffraction pattern. Of the five tested phytopathogens, the pathogens *Phytophthora capsici, Colletotrichum acutatum* and *Cladosporium fulvum* showed 8, 11 and 16 mm zones of inhibition against synthesized silver oxide nanoparticles at 200 µg/well, respectively.

Key words: Silver oxide, nanoparticle, antifungal, plant pathogen, optimization.

INTRODUCTION

Metallic silver has gained much attention for its greener and faster synthesis approaches as well as biomedical, industrial and pharmaceutical applications. It has important chemical, thermal and photo catalytic properties. Physical and chemical methods have been employed to synthesize metal nanoparticles, but these

*Corresponding author. E-mail: ssivaphd@yahoo.com. Tel: +82-55-350-5431. Fax: +82-55-350-5439.

Figure 1. Jackfruit whole tree, rind, rind powder, and the presence of silver nanoparticle confirmation by color change in the reaction mixture.

are hazardous, toxic and expensive (Velmurugan et al., 2016). Hence, the scientific community has turned their attention towards low cost and eco-friendly synthesis of silver nanoparticles from biological sources like plants and microbes (Lee et al., 2016). The bio- and phyto-synthesized silver nanoparticles are non-toxic, ecofriendly and viable. Leaves, fruits, stems, roots, bark and latex have all been used to prepare metallic nanoparticles (Nazeruddin et al., 2014).

Silver nanoparticles with unique physical, chemical and biological properties are certainly the most extensively used nanoparticles in wound dressings, antimicrobial coatings, anti-cancer chemotherapy and cosmetics (Kim et al., 2012). Silver exhibits multiple modes of inhibitory action against microorganisms, which has been used for several years. Silver nanoparticles are common antimicrobial agents because their production costs are low (Lamsal et al., 2011).

According to literature, silver nanoparticles were synthesized from *Tribulus terrestris* (Mariselvam et al., 2014), *Pistacia atlantica* (Sadeghi et al., 2015), *Calotropis procera* (Gondwal and Pant, 2013), *Musa paradisiacal* (Bankar et al., 2010), *Citrus sinensi* (Kaviya et al., 2011), *Eucalyptus hybrid* (Dubey et al., 2009), *Vitis vinifera* (Gnanajobitha et al., 2013) and *Carica papaya* (Jain et al., 2009). Here, the fruit rind extract of jackfruit (Figure 1) was used for the eco-friendly synthesis of silver nanoparticles. *Artocarpus heterophyllus* (Jackfruit tree) is well known as the largest tree-borne fruit. It belongs to the mulberry family, *Moraceae*. However, there is no report on using jackfruit rind to prepare silver nanoparticles.

MATERIALS AND METHODS

Preparation of jackfruit rind extract

The whole jackfruit rind was washed several times with distilled water to remove dirt or uncoordinated materials present on the peel. Then, 100 g of jackfruit rind was cut into small pieces, shade dried and powdered. The 50 g of dried powder was boiled in 250 ml of sterile nanopure water in a 500 mL Erlenmeyer flask for 30 min at 80°C to obtain the peel extract followed by filtration (Whatman No. 42) and stored at 4°C in the refrigerator for future experimental use.

Synthesis of silver oxide nanoparticles

For synthesis of silver oxide nanoparticles (Ag_2O NPs), the jackfruit rind extract (10 mL) was added to 90 mL of 1 mM silver nitrate solution in 250-ml Erlenmeyer flasks to form a reaction mixture, and the reaction was performed under ambient conditions. The reaction mixture was observed for color change from light yellow to dark brown and confirmation of silver nanoparticle synthesis is shown in Figure 1. The intensity of the color was measured using a UV-visible spectrophotometer (UV-1800, UV-Vis spectrophotometer, Shimadzu, Kyoto, Japan) within a working wavelength range of 200 to 800 nm using a dual beam operated at 1 nm resolution).

Optimization of Ag_2O NPs productions

To optimize the nanoparticle production, parameters such as pH of 3, 4, 5, 6, 7, 8, 9 and 10, fruit rind extract at various concentrations of 0.5, 1, 1.5, 2, 2.5, 3, 3.5, 4, 4.5 and 5%, Ag^+ at 0.1, 0.2, 0.3, 0.4, 0.5, 0.6, 0.7, 0.8, 0.9 and 1.0 mM concentrations and reaction times of 0, 15, 30, 45, 60, 75, 90, 105, 120, 135, 150, 165, 180, 195, 210, 240, 270 min were tested. Once the silver nanoparticle production was completed, it was centrifuged at 12,000 rpm for 15 min followed by several washes with copious amounts of nanopure water and ethanol to ensure better separation of free entities from the silver nanoparticle. The product was freeze-dried to make a powder and used for further characterization and antifungal studies.

Characterization of Ag_2O NPs

For characterization, Fourier transform infrared (FTIR) spectra of the phytoconstituents and silver nanoparticles were obtained using a Perkin-Elmer FTIR spectrophotometer (Norwalk, CT, USA) in the diffuse reflectance mode at a resolution of 4 particles cm^{-1} in KBr pellets. High resolution-transmission electron microscopy (HR-TEM model, JEOL-2010, Japan) was used to examine the surface morphology and size of the silver nanoparticles. X-ray powder diffraction of the nanoparticle was obtained using a Rigaku X-ray diffractometer (XRD, Rigaku, Japan).

Antifungal activity of Ag_2O NPs against plant pathogenic fungi

The antifungal activity of Ag_2O NPs, bulk metal silver, rind extract,

Ag_2O NPs blend with rind extract, and standard antifungal (nystatin) were determined by a well diffusion method against the plant pathogenic fungi, viz., *Phytophthora capsici* (KACC 40475), *Phytophthora drechsleri* (KACC 40190), *Didymella bryoniae* (KACC 40900), *Colletotrichum acutatum* (KACC 40042) and *Cladosporium fulvum* (KCCM 11466) obtained from Korean Agricultural Culture Collection (KACC) and maintained in a potato dextrose agar (Ingredients Gms/Litre Potatoes, infusion from 200 g/L, Dextrose 20 g/L, Agar 15 g/L, final pH (at 25°C) 5.6±0.2) cultured in potato dextrose agar medium. The agar wells were made using a sterile juice straw with 5 mm distance to the edge of the plate. The wells were impregnated with Ag_2O NPs at concentrations of 20, 40, and 80 µg/well, bulk metal silver (80 µg/well), gum solution (20 µl/well), and Ag_2O NPs blend with extract (20 µl/well). All fungal isolates were individually inoculated on sterile PDA medium with a 6 mm cork borer in two edge of the Petri plate. The antifungal activities of the jackfruit rind extract and the Ag_2O NPs were determined according to Velmurugan et al. (2016).

RESULTS AND DISCUSSION

The jackfruit (*A. heterophyllus*) rind extract mediated silver nanoparticle fabrication was achieved by adding 1 mM silver ion complex ($AgNO_3$). Next, the aqueous solution was slowly reduced with a color change from light yellow to dark brown (Figure 1) over 20 min in room temperature. The presence of silver nanoparticles was confirmed (Chauhan et al., 2011). The surface plasmon was at 428 nm for the room temperature reaction (Kamat et al., 1998; Rani and Rajasekharreddy, 2011; Gnanajobitha et al., 2013). The common silver nanoparticles synthesis depends on nucleation and growth mechanism (Rai et al., 2006; Fayaz et al., 2009; Song and Kim, 2009; Kaviya et al., 2011). *The* UV–Vis spectra for the formation of silver nanoparticles at different pH values are *shown in Figure 2a. The pH plays a key role in nanoparticle formation.* The shape and size of the nanoparticles are dependent on the pH of the solution. In this study, the absorbance band increased while the pH increased from 4 to 9 for silver nanoparticles. A lower and broader absorbance in silver nanoparticles was observed at lower pH values versus higher pH, this could be due to the larger size of the NPs at lower pH. It has been shown that pH affects the shape and size of a nanoparticles and influences the synthetic process used to make silver nanoparticles (Dwivedi and Gopal, 2010; Vanaja et al., 2013). The results suggest that acidic pH suppresses nanoparticles formation due to increased precipitation or agglomeration due to the instability of the nanoparticles (or the lack of a stabilizing agent). Earlier, Velmurugan et al. (2014a) reported that at a lower pH, agglomeration occurs due to the over-nucleation and formation of larger size nanoparticles. Conversely, at a high pH, many nanoparticles with smaller surface areas are present due to the bioavailability of functional groups in the pine gum solution. Figure 2b shows the UV-Vis spectra of the synthesized silver nanoparticles with different concentrations of jackfruit rind extract (1 to 10%) at 2 mM $AgNO_3$. The peak absorbance consistently increased with increases in the jackfruit rind extract (in 50 mL of 2 mM Ag^+ solution) from 1 to 10% (Figure 2b). These results indicate that more reduction was achieved with jackfruit rind extract concentrations of 2 mL. When the jackfruit rind extract concentration increased, fewer silver nanoparticles were reduced as seen in the spectral peaks in Figure 2c. These results corroborate Pal et al. (2007), Kora et al. (2010) and Velmurugan et al. (2014b) who studied gum acacia, gum kondagogu and pine gum, respectively. The silver ion concentrations were also modulated. The maximum peak absorbance (using UV-Vis) was found for 1.0 mM silver ion with good production (Figure 2c). This could be caused by an enhancement in the oxidation of hydroxyl groups by the metal ions (Kora et al., 2010). The highest yield was observed at 180 min (Figure 2d).

FT-IR analysis (Figure 3) of both jackfruit rind powder extract and silver nanoparticles was done from 4000 to 500 cm^{-1} (Basavegowda and Lee, 2013). The FT-IR spectrum of the water extract of jackfruit rind showed absorptions at the following peaks: 3438 cm^{-1} representing the -OH group; 2931 cm^{-1} assigned to the stretching vibration of C-H methyl and methylene bond; 1743 cm^{-1} assigned to the C=O stretching of pectin ester and carboxylic acid; and 1613 cm^{-1} attributed to the C=O stretching of carboxylic acid with intermolecular hydrogen bond. The peaks at 1422, 1058 and 629 cm^{-1} were assigned to symmetric bending of CH_3, -SO3 and C-O stretching of ether groups, respectively. The FTIR spectrum of the Ag_2ONPs synthesized using jackfruit rind extract shows different bands at 3408, 2922, 1613, 1383, 1020 and 610 cm^{-1}. Upon comparing the FTIR spectra of the extract and Ag_2O NPs, there was a shift in the bands of the carbonyl and hydroxyl groups. This indicates that the major bio-molecules from the extract were capped on the Ag_2O NPs surface and shows their characteristic peaks in the IR spectrum of the silver solution.

HR-TEM was used to study the shape and size of the Ag_2O NPs obtained via jackfruit rind extracts. The HR-TEM image (Figure 4a) shows Ag_2O NPs (11.2 to 24.5 nm) with an abundance of roughly spherical Ag_2O NPs. The selected area electron diffraction (SAED) pattern of Ag_2O NPs is shown in Figure 4b. The bright circular rings in the SAED pattern confirm the crystallinity of the Ag_2O NPs prepared from jackfruit. Some of the nanoparticles do not have a smooth surface morphology due the presence of both individual and agglomerated Ag_2O NPs.

The powder X-ray diffraction of the Ag_2O NPs is shown in Figure 4c. This confirms the presence of genuine silver (I) oxide nanoparticles. The XRD spectra confirmed the standard spectra of Ag_2O (JCPDS no. 00-012-0793). Many Bragg reflection peaks were observed at 2θ values of 32.03, 40.01, 55.02, 65.03 and 77.45°. These are indexed to (111), (111), (200), (220), (220) and (222) planes of pure Ag_2O NPs and match that of the standard spectra of silver (JCPDS no.# 00-004-0783), silver (II) oxide (JCPDS no.# 00-012-0793), and silver oxide

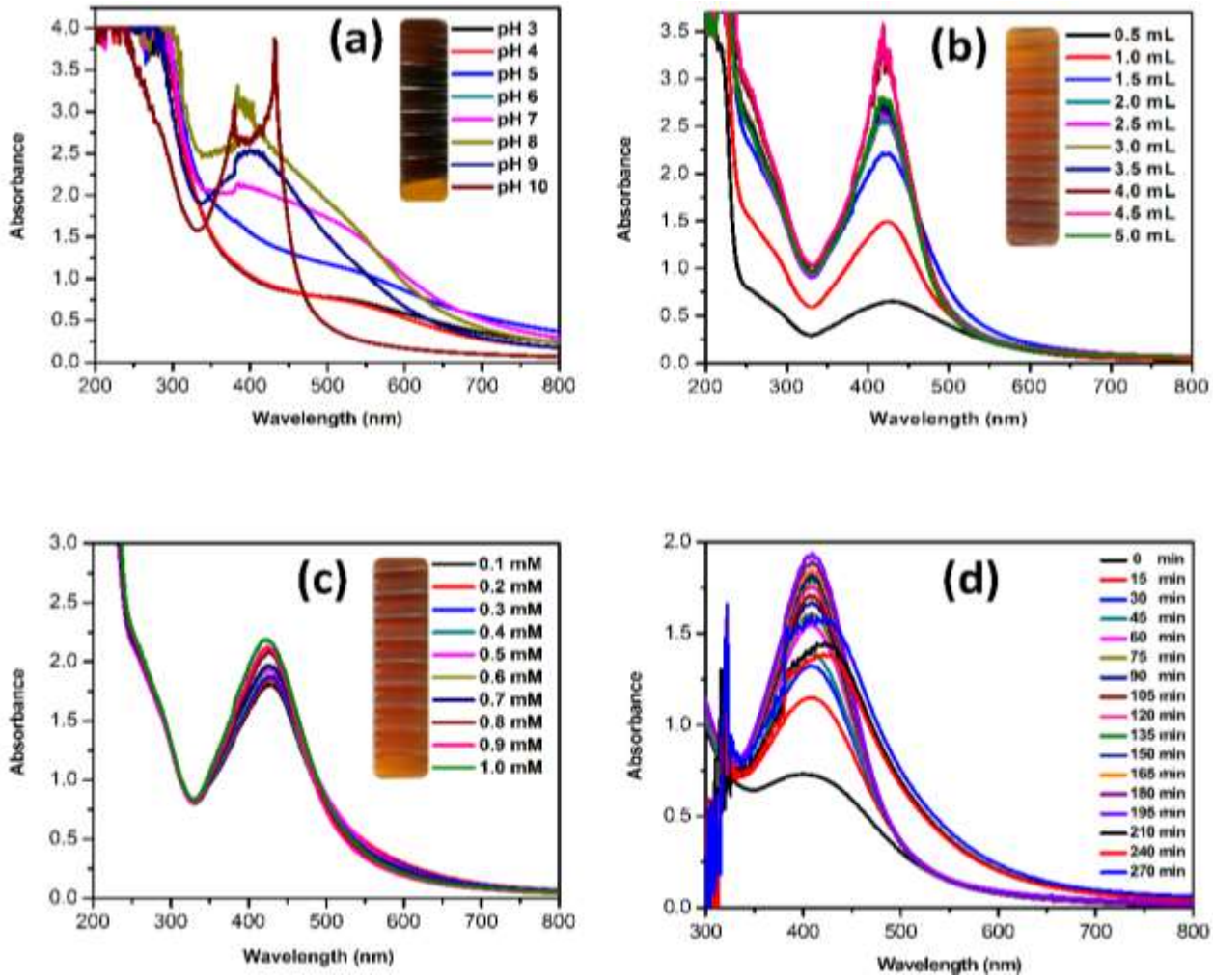

Figure 2. UV–Vis absorption spectra of optimizing parameters to produce Ag_2O NPs with different pHs: (a) ratios of jackfruit rind extract from 0.5 to 5 mL (b), concentration of metal ions Ag^+ from 0.1 to 1.0 mM (c) and times from 0 to 270 min (d).

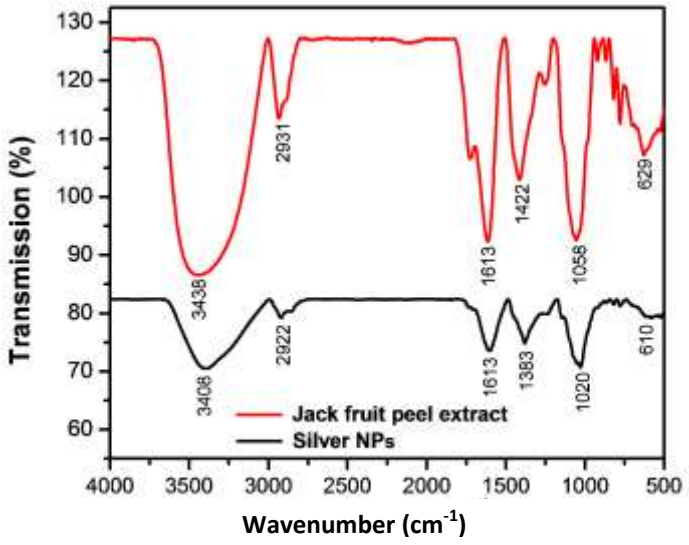

Figure 3. FTIR spectra of the jackfruit rind extract powder and the Ag_2O NPs synthesized at optimum parameters.

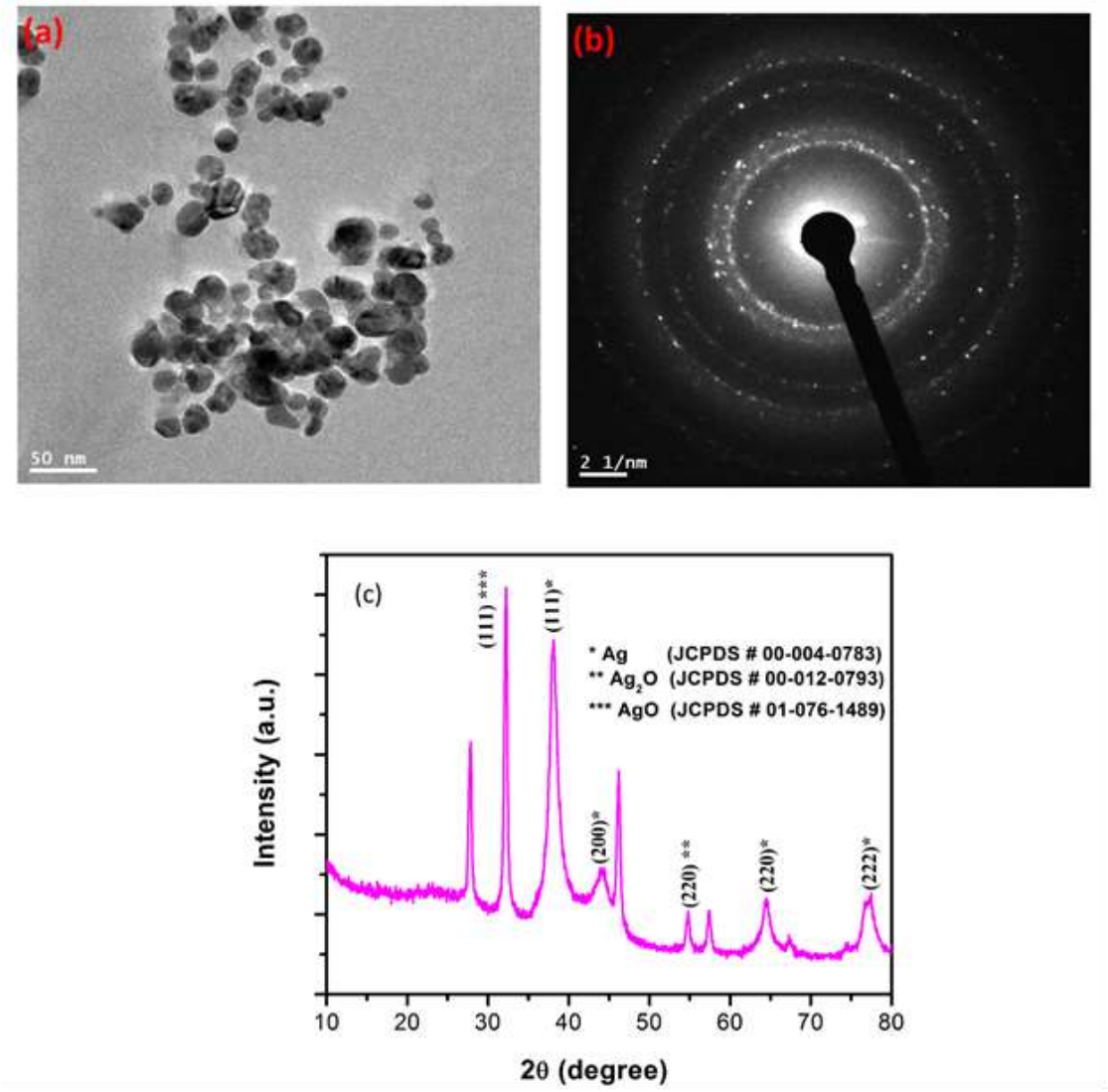

Figure 4. TEM images of Ag_2O NPs (a) 24.2 nm, corresponding SAED pattern for Ag_2O NPs (b) and (c) XRD patterns of the Ag_2O NPs synthesized at the optimum parameters.

(JCPDS no.# 01-076-1489) (Velmurugan et al., 2016). The XRD analysis confirms the face-centered cubic (FCC) configuration of biosynthesized Ag_2O NPs. This used PANalytical X'Pert HighScore Plus software, Version 3.0.3 (Figure 5). The mean particle diameter of Ag_2O NPs was calculated from the XRD pattern using the Scherrer equation:

$D = K\lambda/\beta_{1/2}$ COS θ.

Here, K is the shape constant, λ is the wavelength of the X-ray, $\beta_{1/2}$ and u are the half width of the peak and half of the Bragg's angle, respectively. The calculated average crystallite size of the Ag_2O NPs was 24.2 nm from the breadth of the (111) reflection.

The *in vitro* antifungal activity of synthesized Ag_2O NPs versus a commercially available antifungal agent was carried out for the first time against five different plant pathogenic fungi. The Ag_2O NPs and a combination of extract and Ag_2O NPs showed remarkable activity against four plant pathogenic fungi, *C. acutatum, P. capsici*, *P. drechsleri* and *C. fulvum* (Table 1). The *P. drechsleri* showed resistance to the commercial antifungal agent, nystatin (20 µg/well); however, *D. bryoniae,* were resistant to synthesized Ag_2O NPs (Table1).

Conclusions

In summary, jackfruit rind extract mediated Ag_2O NPs synthesis is a simple technique that contributes to the area of green synthesis and nanotechnology. It has no

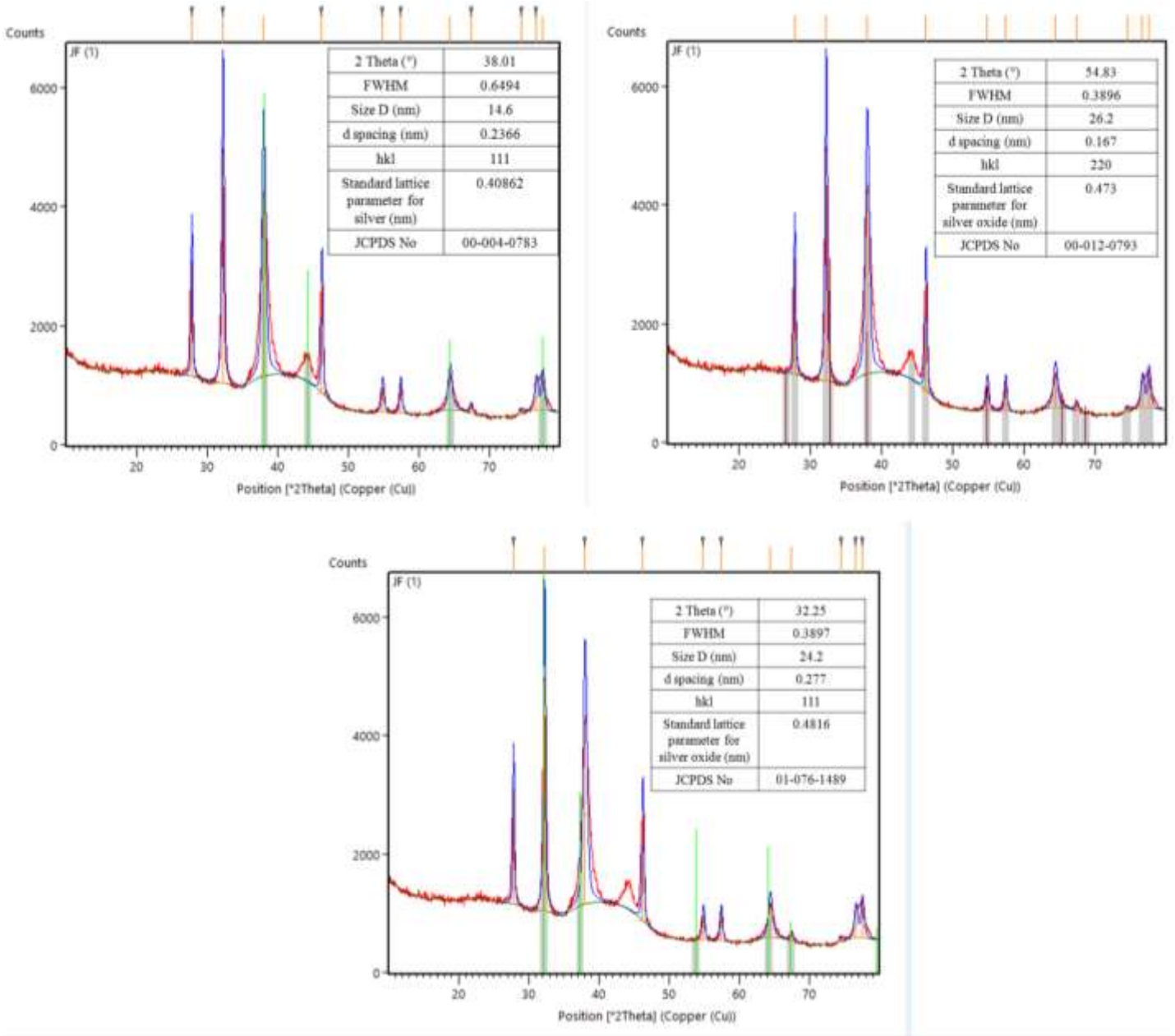

Figure 5. Mean particle diameter of Ag_2O NPs calculated from the XRD pattern using the Scherrer equation.

Table 1. Zone of inhibition (mm) of synthesized Ag_2O NPs and blend of extract with Ag_2O NPs against plant fungal pathogens.

S/N	Strains	Zone of inhibition (ZOI) in mm						
		Ag_2O NPs + extract (µL)			Synthesized Ag_2O NPs (µg)			Control
		25	50	100	100	150	200	
1.	*C. acutatum*	2	4	5	5	8	11	22
2.	*P. capsici*	2	3	6	4	6	8	24
3.	*P. drechsleri*	3	4	6	4	6	10	No zone
4.	*C. fulvum*	2	6	8	8	12	16	22
5.	*D. bryoniae*	No zone	No zone	No zone	No zone	No zone	No zone	24

external chemicals or physical steps. This study showed the efficiency of Ag_2O NPs synthesized by jackfruit rind extracts. This is an environmentally benign method to prepare metal oxide nanoparticles. The product's physical characteristics were analyzed with UV-Vis spectroscopy, FTIR, XRD, techniques and TEM. The Ag_2O NPs were monodisperse, spherical and 10 and 30 nm in diameter. The antifungal activity of Ag_2O NPs was investigated against a plant pathogenic fungus, and it shows moderate to good activity with few pathogens. Based on these findings, this method is suitable for the industrial scale production of Ag_2O NPs from a commonly discarded waste jackfruit rind.

CONFLICT OF INTERESTS

The authors did not declare any conflict of interest.

ACKNOWLEDGEMENT

This work was supported by a 2 Years Research Grant of Pusan National University.

REFERENCES

Bankar A, Joshi B, Kumar AR, Zinjarde S (2010). Banana peel extract mediated synthesis of gold nanoparticles. Colloids Surf. B. 80:45-50.

Basavegowda N, Lee YR (2013). Synthesis of silver nanoparticles using Satsuma mandarin (*Citrus unshiu*) peel extract: A novel approach towards waste utilization. Mater. Lett. 109:31-33.

Chauhan S, Upadhyay MK, Rishi N, Rishi S (2011). Phyto fabrication of silver nanoparticles using pomegranate fruit seeds. Int. J. Nanomater. Biostruct. 1:17-21.

Dubey M, Bhadauria S, Kushwah BS (2009). Green synthesis of nanosilver particles from extract of *Eucalyptus hybrida* (safeda) leaf. Dig. J. Nanomater. Biostruct. 4:537-543.

Dwivedi AD, Gopal K (2010). Biosynthesis of silver and gold nanoparticles using *Chenopodium album* leaf extract. Colloids Surf. A Physicochem. Eng. Asp. 369:27-33.

Fayaz AM, Balaji K, Kalaichelvan PT, Venkatesan R (2009). Fungal based synthesis of silver nanoparticles—an effect of temperature on the size of particles. Colloids Surf. B Biointerfaces 74:123-126.

Gnanajobitha G, Paulkumar K, Vanaja M, Rajeshkumar S, Malarkodi C, Annadurai G, Kannan C (2013). Fruit-mediated synthesis of silver nanoparticles using *Vitis vinifera* and evaluation of their antimicrobial efficacy. J. Nanostructure Chem. 3:67.

Gondwal M, Pant GJN (2013). Biological evaluation and green synthesis of silver nanoparticles using aqueous extract of *Calotropis procera.* Int. J. Pharm. Biol. Sci. 4:635-643.

Jain D, Daima HK, Kachhwaha S, Kothari SL (2009). Synthesis of plant-mediated silver nanoparticles using papaya fruit extract and evaluation of their anti-microbial activities. Dig. J. Nanomater. Biostruct. 4:557-563.

Kamat PV, Flumiani M, Hartland GV (1998). Picosecond dynamics of silver nanoclusters. Photoejection of electrons and fragmentation. J. Phys. Chem. B 102:123-3128.

Kaviya S, Santhanalakshmi J, Viswanathan B, Muthumary J, Srinivasan K (2011). Biosynthesis of silver nanoparticles using citrus sinensis peel extract and its antibacterial activity. Spectrochim. Acta A Mol. Biomol. Spectrosc. 79:594-598.

Kim SW, Jung JH, Lamsal K, Kim YS, Min JS, Lee YS (2012). Antifungal effects of silver nanoparticles (AgNPs) against various plant pathogenic fungi. Mycobiology 40:53-58.

Kora AJ, Sashidhar RB, Arunachalam J (2010). Gum kondagogu (*Cochlospermum gossypium*): a template for the green synthesis and stabilization of silver nanoparticles with antibacterial application. Carbohydr. Polym. 82:670-679.

Lamsal K, Kim SW, Jung JH, Kim YS, Kim KS, Lee YS (2011). Application of silver nanoparticles for the control of *Colletotrichum* species *in vitro* and pepper anthracnose disease in field. Mycobiology 39:194-199.

Lee JH, Lim JM, Velmurugan P, Park YJ, Park YJ, Bang KS, Oh BT (2016). Photobiologic-mediated fabrication of silver nanoparticles with antibacterial activity. J. Photochem. Photobiol. 162:93-99.

Mariselvam R, Ranjitsingh AJA, Nanthini AUR, Kalirajan K, Padmalatha C, Selvakumar PM (2014). Green synthesis of silver nanoparticles from the extract of the inflorescence of *Cocos nucifera* (Family: *Arecaceae*) for enhanced antibacterial activity. Spectrochim. Acta Mol. Biomol. Spectrosc. 129:537-541.

Nazeruddin GM, Prasad NR, Waghmare SR, Garadkar KM, Mulla IS (2014). Extracellular biosynthesis of silver nanoparticle using *Azadirachta indica* leaf extract and its anti-microbial activity. J. Alloys Compd. 583:272-277.

Pal S, Tak YK, Song JM (2007). Does the antibacterial activity of silver nanoparticles depend on the shape of the nanoparticle? A study of the gram-negative bacterium *Escherichia coli.* Appl. Environ. Microbiol. 73:1712-1720.

Rai A, Singh A, Ahmad A, Sastry M, (2006). Role of halide ions and temperature on the morphology of biologically synthesized gold nanotriangles. Langmuir 22:736-741.

Rani PU, Rajasekharreddy P (2011). Green synthesis of silver-protein (core–shell) nanoparticles using *Piper betle* L. leaf extract and its ecotoxicological studies on *Daphnia magna.* Colloids Surf. A Physicochem. Eng. Asp. 389:188-194.

Sadeghi B, Rostami A, Momeni SS (2015). Facile green synthesis of silver nanoparticles using seed aqueous extract of *Pistacia atlantica* and its antibacterial activity. Spectrochim. Acta Mol. Biomol. Spectrosc. 134:326-332.

Song JY, Kim BS (2009). Rapid biological synthesis of silver nanoparticles using plant leaf extracts. Bioprocess Biosyst. Eng. 32:79-84.

Vanaja M, Rajeshkumar S, Paulkumar K, Gnanajobitha G, Malarkodi C, Annadurai G (2013). Phytosynthesis and characterization of silver nanoparticles using stem extract of *Coleus aromaticus.* Int. J. Mater. Biomater. Appl. 3:1-4.

Velmurugan P, Lee SM, Cho M, Park JH, Seo SK, Myung H, Bang KS, Oh BT (2014 a). Antibacterial activity of silver nanoparticle-coated fabric and leather against odor and skin infection causing bacteria. Appl. Microbiol. Biotechnol. 98:8179-8189.

Velmurugan P, Cho M, Lee SM, Park JH, Bae S, Oh BT (2014b). Antimicrobial fabrication of cotton fabric and leather using green-synthesized nanosilver. Carbohydr. Polym. 106:319-325.

Velmurugan P, Shim J, Kim K, Oh BT (2016). *Prunus*× *yedoensis* tree gum mediated synthesis of platinum nanoparticles with antifungal activity against phytopathogens. Mater. Lett. 174:61-65.